Model Energy Landscapes and the Force-Induced Dissociation of Ligand-Receptor Bonds

T. Strunz, K. Oroszlan, I. Schumakovitch, H.-J. Güntherodt, and M. Hegner
Department of Physics and Astronomy, University of Basel, 4056 Basel, Switzerland

ABSTRACT   We discuss models for the force-induced dissociation of a ligand-receptor bond, occurring in the context of cell adhesion or single molecule unbinding force measurements. We consider a bond with a structured energy landscape which is modeled by a network of force dependent transition rates between intermediate states. The behavior of a model with only one intermediate state and a model describing a molecular zipper is studied. We calculate the bond lifetime as a function of an applied force and unbinding forces under an increasing applied load and determine the relationship between both quantities. The dissociation via an intermediate state can lead to distinct functional relations of the bond lifetime on force. One possibility is the occurrence of three force regimes where the lifetime of the bond is determined by different transitions within the energy landscape. This case can be related to recent experimental observations of the force-induced dissociation of single avidin-biotin bonds.

INTRODUCTION

Cell adhesion is mediated by the specific interaction between ligands and receptors which form weak noncovalent bonds. The reaction kinetics of ligands and the receptors that are both confined to cell membranes are therefore essential for the kinetics and mechanics of the cell adhesion process (Zhu, 2000; Bongrand, 1999). One important aspect of ligand-receptor interaction in an adhesion context is that bonds are formed or broken under the influence of a mechanical force. Whereas the formation of a bond is strongly influenced by steric factors, the breaking of a bond, i.e., the dissociation kinetics under a mechanical force, is an intrinsic property of the ligand-receptor complex.

Recent experiments allowed us to measure the mechanical unbinding of single ligand-receptor complexes directly with atomic force microscopy (AFM) (Florin et al., 1994; Lee et al., 1994a,b; Moy et al., 1994; Dammer et al., 1995, 1996; Hinterdorfer et al., 1996, 1998; Allen et al., 1997) or bio-membrane force probes (Evans et al., 1995). In these experiments the force at which a complex unbinds when loaded with a force ramp (increasing from zero) is measured (Fig. 1 A). This unbinding force is directly related to the dissociation kinetics of the complex under an applied force and therefore depends on the loading rate (the rate of force increase before the unbinding) (Evans and Ritchie, 1997). In principle, it is possible to determine the dissociation rate, or the lifetime, of a bond in function of the mechanical force on the complex from loading rate-dependent measurements of the unbinding force (a method termed dynamic force spectroscopy) (Evans, 1998; Fritz et al., 1998; Merkel et al., 1999; Strunz et al., 1999; Simson et al., 1999; Williams et

al., 2000). Interestingly, all ligand-receptor systems investigated so far show an exponential increase of the dissociation rate with force in the limit of small forces, as originally stated by Bell (Bell, 1978). This leads to a linear dependence of the unbinding force on the logarithm of the loading rate. A similar behavior is also observed for the mechanical unfolding of proteins (Rief et al., 1997; Carrion-Vazques et al., 1999). This can also be viewed as a linear decrease of the free energy for dissociation, which is expected for a single sharp energy barrier along the dissociation path (Fig. 1 B). However, there are also a number of ligand-receptor systems that show deviations from this behavior for larger forces, which is attributed to the internal structure of their energy landscape (Evans, 1998; Merkel et al., 1999).

To answer the question of how the structure of the energy landscape influences the dissociation kinetics under applied force and, conversely, what can be learned about the internal structure of ligand-receptor bonds by dynamic force spectroscopy (DFS), we discuss models for the dissociation kinetics of complexes with a structured energy landscape. A structured energy landscape basically means that the dissociation proceeds via intermediate bound states and/or that several transition states to the unbound state exist. These can be described by a network of (force-dependent) transition rates between the states. This approach is complementary to detailed molecular dynamic simulations of the forced unbinding of a complex (Grubmüller et al., 1996; Izrailev et al., 1997; Haymann and Grubmüller, 1999), where the time scale of the unbinding is several orders of magnitude faster (the bond lifetimes are in the nanosecond range) than the experimentally accessible time scale (lifetimes from several seconds to milliseconds). The dependence of the unbinding force on the logarithm of the loading rate, which is characteristic for the thermally activated process, is not captured by the molecular dynamic simulations. If the molecular dynamic trajectories are representative for the unbinding pathway of the complex on the experimental time scale one
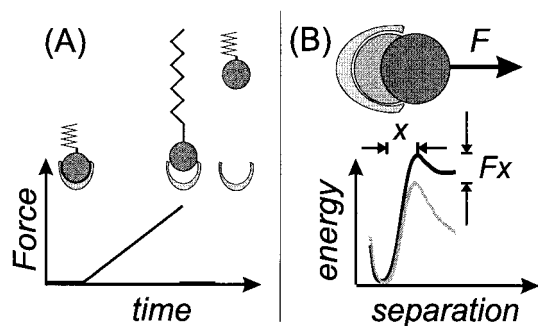
FIGURE 1 (*A*) Direct observation of the dissociation under a mechanical force. The force on a single complex increases until it dissociates. The dissociation is monitored by an abrupt relaxation of the macroscopic spring of a force probe. (*B*) The dissociation over a sharp energy barrier is characterized by a linear decrease of the barrier with applied force *F*, giving rise to a characteristic length scale *x*.

is in principle able to construct an energy landscape from the simulations (Balsera et al., 1997; Gullingsgud et al., 1999). Such an energy landscape could be used to identify appropriate intermediate states and transition rates.

In a further approximation we restrict ourselves to models where the transition rates between different intermediate states depend only exponentially on the force, i.e., the intermediate states are separated by sharp energy barriers. This approximation neglects changes in the geometry of the transition state by the mechanical force and changes in the friction the complex experiences along the separation path.

It is clear that the dissociation process in such a network of intermediate states may strongly depend on the applied force, because completely different transitions may dominate the dissociation kinetics at different forces. In this work we discuss, among the many possible network topologies of intermediate states, a model with one intermediate state along the separation pathway (Fig. 2 *A*). Aside from representing the most simple situation the model can describe some observations in recent DFS measurements (Evans, 1998; Merkel et al., 1999). As a second example we discuss the model of a symmetrically loaded molecular zipper (Fig. 2 *B*), describing recent DFS measurements on the mechanical dissociation of DNA (Strunz et al., 1999). In both cases we discuss the complex lifetime as function of force, the distributions of unbinding forces at different loading rates, the most probable unbinding force as a function of loading rate (observable in a DFS experiment), and an approximation to the lifetime derived from the last function.

DISSOCIATION KINETICS UNDER AN APPLIED FORCE

First we briefly review the basic model for dissociation kinetics of a ligand-receptor complex subject to a dislodging force *F* which is described by an exponential increase of the
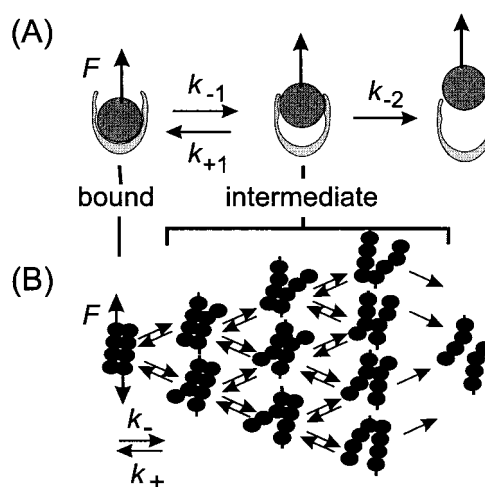

FIGURE 2 Reaction schemes for the dissociation kinetics. (*A*) Dissociation via an intermediate state. (*B*) Transition scheme of the zipper model.

dissociation rate:

$$k_d(F) = k_d(0)e^{Fx/kT}, \tag{1}$$

where *kT* is the thermal energy. The exponential increase is characteristic for a sharp energy barrier where the transition state is located at a distance *x*, projected along the direction of applied force, to the ground state (Fig. 1 *B*). In this situation the free energy for dissociation decreases linearly with the applied force, i.e., $\Delta G^{\#}(F) = \Delta G^{\#} - Fx$, with $k_d(0) = (kT/h)e^{-\Delta G^{\#}/kT}$ and *h* is the Planck constant.

The behavior of this model in the context of an unbinding force measurement, where the force increases until the complex unbinds, has been discussed in detail by Evans and Ritchie (1997). For the sake of simplicity we assume here that the force on the complex increases with a constant loading rate *r*. Generally the force on a complex does not increase linearly with time in most experimental systems and likely also not in biological situations. The approximation of a constant loading rate is nevertheless good with a properly determined effective loading rate (Evans and Ritchie, 1999). Because the measurement is done with a soft spring, ligand and receptor are further separated after crossing the transition state and rebinding will be neglected. The stochastic nature of the unbinding events is captured by solving the master equation for the probability *N(t)* to be in the bound state under an increasing load $F = rt$:

$$\frac{dN(t)}{dt} = -k_d(rt)N(t). \tag{2}$$

This results in a distribution of unbinding forces $P(F) = r^{-1}k_d(F)N(F/r)$ (with $N(0) = 1$) which with Eq. 1 is given by:

$$P(F) = k_d(0)r^{-1}e^{Fx/kT + k_d(0)r^{-1}kT/x(1 - e^{Fx/kT})}. \tag{3}$$

The most probable unbinding force F^*, the maximum of the distribution, is given by

$$F^* = \frac{kT}{x} \ln \frac{r}{k_d(0)\frac{kT}{x}}. \tag{4a}$$

In this case the parameters governing the dissociation kinetics under an applied force, the thermal dissociation rate $k_d(0)$ and the length scale x, can be determined directly from a plot of the most probable unbinding force versus the logarithm of the loading rate. Note that Eq. 4a, because of Eq. 1, can be rewritten to:

$$k_d(F^*) = rkT/x. \tag{4b}$$

The distribution of Eq. 3 is an extreme-value type distribution (Abramowitz and Stregun, 1972, Eq. 26.1.30) that can be rewritten in terms of the most probable unbinding force F^* as

$$P(F) = ae^{(F-F^*)x/kT - e^{(F-F^*)x/kT}},$$

with $a = (x/kT)e^{e^{-F^*x/kT}}$. In general the dissociation might proceed via intermediate states and it is also possible that multiple transition states exist. This situation is captured by the generalized master equation:

$$\frac{d\mathbf{N}(t)}{dt} = -\mathbf{k_d}(F)\mathbf{N}(t), \tag{5}$$

where $\mathbf{N}$ is a vector which components N_i represent the occupation probabilities of each bound state and $\mathbf{k_d}(F)$ is a matrix describing the transitions between the states and to the unbound state. Although there are now multiple time scales in the system we can define an effective dissociation rate by the inverse of the mean dissociation time τ at fixed force F given by

$$\tau(F) = \int_0^\infty t \frac{dN_u}{dt} dt, \tag{6}$$

where $N_u = 1 - \Sigma_i N_i(t)$ is the probability to be in the unbound state. N_u is calculated from a solution of Eq. 5 (by calculating the eigenvalues of $\mathbf{k_d}(F)$) with the initial condition that the probability of the complex being in the ground state is one and the other states are occupied with zero probability (Anshelevich et al., 1984).

The distribution of unbinding forces for a given loading rate r is derived from the generalized solution of Eq. 2, i.e., the solution of Eq. 5 with $F = rt$, resulting in a function $\tilde{N}_u$ and

$$P(F) = r^{-1} \frac{d\tilde{N}_u}{dt}\bigg|_{t=F/r}. \tag{7}$$

In general, a model for the dissociation process like Eq. 5 is necessary to connect the unbinding forces measured in a DFS experiment (given by Eq. 7) with the dissociation time in Eq. 6. However, if we have determined the most probable unbinding force F^* in dependence of the loading rate, we can estimate the dissociation time as a function of the force by approximating the measured function $F^*(\ln(r))$ linearly at every loading rate. Using Eq. 4b to estimate $k_d(F^*)$, with the local slope $kT/x = dF^*/d\ln(r)$, gives an estimate of the mean dissociation time $\tau(F)$ in a general situation:

$$\tau_e(F^*) \approx \frac{dF^*}{dr}. \tag{8}$$

For the examples we discuss below, we find that this approximation is appropriate when the local slope of the F^* vs. $\ln(r)$ curve does not change too rapidly with the loading rate.

FORCED DISSOCIATION WITH AN INTERMEDIATE STATE

In the two-barrier model, the dissociation proceeds via an intermediate state. We assume that all transition rates, namely the transition rate from the ground to the intermediate state $k_{-1}(F)$, the backward rate $k_{+1}(F)$, and the rate from the intermediate to the unbound state $k_{-2}(F)$, depend exponentially on the force, i.e., $k_i(F) = k_i(0)e^{Fx_i/kT}$. The corresponding length scales are x_{-1}, x_{+1} (negative for a transition opposite to the direction of applied force) and x_{-2}, respectively. The mean dissociation time for a fixed force, defined by Eq. 6, is given by

$$\tau(F) = \frac{k_{-1}(F) + k_{+1}(F) + k_{-2}(F)}{k_{-1}(F)k_{-2}(F)}. \tag{9}$$

By this analytic formula we can classify typical cases for the dependence of the effective dissociation rate $\tau^{-1}(F)$ on the force (Fig. 3). Because the intermediate state is energetically located above the ground state we have $k_{+1}(0) \gg k_{-1}(0)$ (assuming an energy difference of a few kT). We first focus on the cases where the transition state from the intermediate to the unbound state has a higher energy than the transition state to the ground state so that $k_{+1}(0) \gg k_{-2}(0)$ also holds (Fig. 3, A and B). In this case the limit of small forces in Eq. 9 leads to the effective dissociation rate

$$\tau^{-1}(F) \approx \frac{k_{-1}(0)k_{-2}(0)}{k_{+1}(0)} e^{F(x_{-1}-x_{+1}+x_{-2})/kT}, \tag{10}$$

so that the exponential increase of the thermal dissociation rate is governed by distance of the ground state to the outermost barrier. With increasing force the backward transition becomes negligible, $k_{-1}(0) \gg k_{+1}(0)$, and the dissociation is dominated by either the transition rate to the intermediate state $k_{-1}(0)$ or to the unbound state $k_{-2}(0)$. It
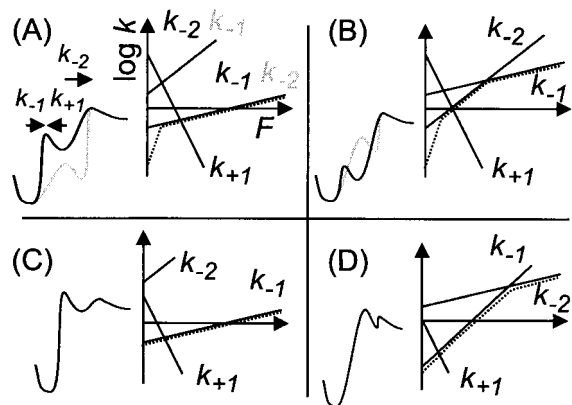
FIGURE 3 Classification of the dissociation behavior via an intermediate state in function of a mechanical force. (*Left*) Schematic energy landscapes. (*Right*) Logarithm of the model transition rates $k_{-1}(F)$, $k_{+1}(F)$ and $k_{-2}(F)$ as function of force. The effective dissociation rate is indicated by a dotted line. The gray potential scheme corresponds to an exchange of the functions $k_{-1}(F)$ and $k_{-2}(F)$ which does not change the effective dissociation rate. (*A*) Two regimes in the dissociation process appear. At small forces all three transitions rates determine the process. At high forces the transition from the ground to the intermediate state (from the intermediate to the unbound state, for the gray potential scheme) is rate determining. (*B*) Similar situation as in *A*, but the rate-determining (forward) transitions cross over with increasing force. (*C* and *D*) The intermediate state is only visited after the transition state with the highest energy has been passed. Because the dynamics of the complex is over-damped and fluctuation-driven, the intermediate can still be dynamically relevant at an applied force (*D*).

is also possible that upon further increase of the force a second transition occurs, where the rate dominating transition changes again (Fig. 3 *B*). If the rate is dominated by the transition from the ground to the intermediate state it can become dominated by the transition from the intermediate to the unbound state upon increasing the force, for example. In this case three force intervals in the dissociation rate occur. For small forces the dissociation rate is given by Eq. 10, in the second interval the dissociation rate is $\approx k_{-1}(F)$ (or $k_{-2}(F)$) and in the third interval $\approx k_{-2}(F)$ (or $k_{-1}(F)$). Only in this case can all parameters describing the two state model (i.e. all three rates and length scales) be extracted directly by measuring the function $\tau(F)$. However, because interchanging the parameters describing the functions $k_{-2}(F)$ and $k_{-1}(F)$ leads to no changes in $\tau(F)$, it is not possible to assign the measured parameters unambiguously to a transition.

In addition to the above cases it is also possible that the transition state from the ground to the intermediate state is the thermodynamically relevant transition state so that $k_{+1}(0) < k_{-2}(0)$ (Fig. 3, *C* and *D*). Nevertheless the intermediate state can be rate determining with an applied force (Fig. 3 *D*).

To discuss the dynamic force spectroscopy of the two-state model we solved the differential Eq. 5 with $F = rt$ numerically with Gear's backward differentiation method

implemented in the IMSL library (IMSL Inc., Houston, TX; see also Press et al., 1992). For specific parameter values we chose, as an example, the values to represent the case with three regimes in the dissociation process (Fig. 3 *B*). The transition rates and length scales were chosen to fit the experimental data of Merkel et al. (1999), where three distinct regimes in the unbinding force vs. loading rate plot for avidin-biotin have been observed. With $k_{-1}(0) = 0.5$ s^{-1}, $x_{-1} = 0.4$ nm, $k_{-2}(0) = 30$ s^{-1} and $x_{-2} = 0.1$ nm the regimes at higher forces could be matched and $k_{+1}(0) = 1.5*10^4$ s^{-1}, $x_{+1} = -2.5$ nm was found to reproduce the behavior at small forces.

Figure 4 *A* shows the most probable unbinding force F^* of the distribution Eq. 7 in dependence of the loading rate. The three regimes where the dissociation is determined by different processes also lead to three different regimes in the unbinding vs. loading rate plot. In the case where we exchanged the parameters describing the forward transitions ($k_{-1}(0) = 30$ s^{-1}, $x_{-1} = 0.1$ nm, $k_{-2}(0) = 0.5$ s^{-1} and $x_{-2} = 0.4$ nm) the distribution of unbinding forces displays two local maxima (Fig. 4 *B*) near a crossover between two regimes: this feature occurs for loading rates where the transition to the intermediate state is the rate determining step and the transition to the unbound state is still not much faster. This leads to the jump in the absolute maximum of the distribution in function of the loading rate. However, in an experiment the maxima would be difficult to detect because of the experimental noise and the limited statistics. We also calculated the mean and the standard deviation of the distribution of unbinding forces in function of the loading rate. Both are steady functions of the loading rate. The mean unbinding force is close to the most probable unbinding force when no jump is present (Fig. 4 *A*). The mean unbinding force and the standard deviation show no significant change in their behavior when the order of the transitions in the binding pocket is changed. Therefore, we would expect that experimentally measured unbinding force distributions would also not be sensitive to the order of the forward transitions in the binding pocket.

Figure 4 *C* shows a comparison between the calculated and estimated dissociation time. Deviations between both occur if the slope of unbinding force vs. log loading rate curve changes rapidly. Nevertheless, Eq. 8 can be used to estimate to a first approximation the dissociation rate as a function of the force by loading rate-dependent unbinding force measurements.

The model with one intermediate state is therefore the simplest model to explain the experimentally observed behavior of the biotin-avidin system. But the actual energy landscape of the bond may still be more complicated because only the rate determining transitions are clearly detectable in the bond lifetime as a function of force (compare Fig. 2 *C*). Generally, the low force regime is always associated with the thermodynamically relevant transition state
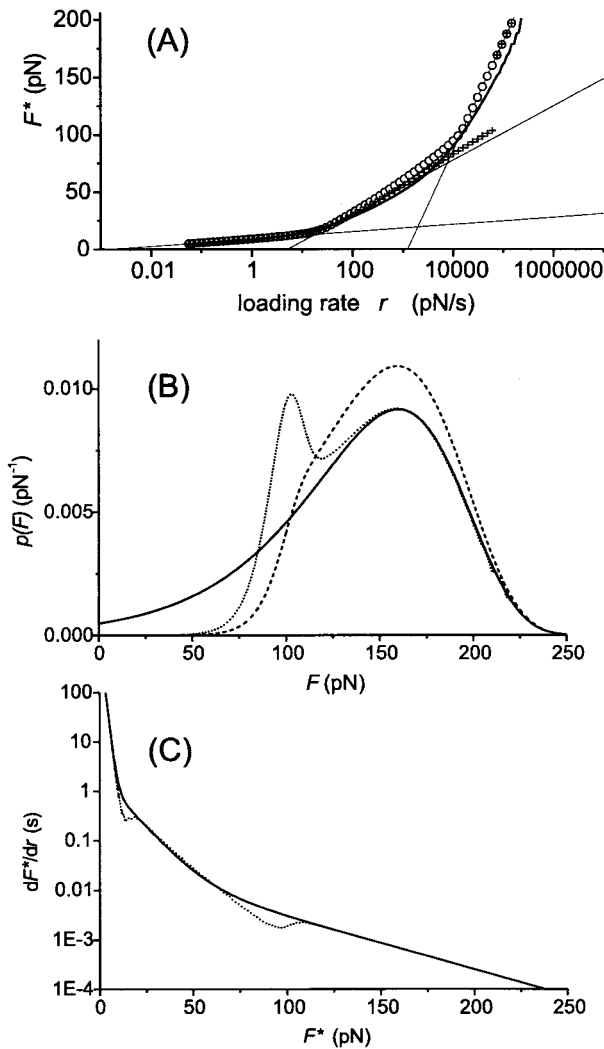
FIGURE 4 (*A*) Calculated loading rate dependence of the most probable unbinding force F^* for a model with one intermediate state (Fig. 2 *A*). Parameters: $k_{+1}(0) = 1.5 \times 10^4 \, \text{s}^{-1}$, $x_{+1} = -2.5$ nm. *Open circles*: $k_{-1}(0) = 0.5 \, \text{s}^{-1}$, $x_{-1} = 0.4$ nm, $k_{-2}(0) = 30 \, \text{s}^{-1}$ and $x_{-2} = 0.1$ nm. *Crosses*: $k_{-1}(0) = 30 \, \text{s}^{-1}$, $x_{-1} = 0.1$ nm, $k_{-2}(0) = 0.5 \, \text{s}^{-1}$, and $x_{-2} = 0.4$ nm. The solid lines indicate the loading rate dependence according to Eq. 4 with $k_{\text{d}}(0) = 1 \times 10^{-3} \, \text{s}^{-1}$ & $x = 3.0$ nm, $k_{\text{d}}(0) = 0.5 \, \text{s}^{-1}$ & $x = 0.4$ nm and $k_{\text{d}}(0) = 30 \, \text{s}^{-1}$ & $x = 0.1$ nm. For the parameters corresponding to the crosses the mean unbinding force of the force distribution is also shown as a solid curve. It does not show the jump that occurs because of the two local maxima of the distribution. (*B*) Distributions of the unbinding force for $r = 6 \times 10^4$ pN/s. *Solid line*: Distribution function according to Eq. 3 for the corresponding F^* and $x = 0.1$ nm. *Dashed (dotted) line*: Distribution corresponding to the open circles (*crosses*) in *A*. (*C*) Approximate mean dissociation time Eq. 8 (*dotted line*, from the data corresponding to the open circles in *A* and mean dissociation time Eq. 9 (*solid line*).

and the corresponding length scale is the distance to the ground state projected along the direction of applied force. The regimes at higher forces correspond to rate determining transitions which can be located anywhere along the mechanical separation pathway.

FORCED DISSOCIATION IN THE ZIPPER MODEL

Inspired by the unbinding force measurements of DNA duplexes pulled at the opposite 5′ ends (Strunz et al., 1999) we investigate the behavior of a zipper model, used to describe the thermodynamic behavior (Pörschke, 1977), under an applied force. The simplest form of the model is described by two rates, one is the rate $k_-(0)$ of opening of a base pair (or a general subunit in zipper type configuration) if the neighboring base pair is already open (hence the term zipper), the other is the rate $k_+(0)$ of closing a base pair neighboring a closed pair (Fig. 2 *B*). We now investigate the model where the force is applied at the opposite ends of the zipper (corresponding to the 5′ end to 5′ end pulling of DNA) so that $k_\pm(F) = k_\pm e^{Fx_\pm/kT}$ (note that x_+ is negative) to a first approximation. The mean dissociation time for a zipper of length n is given by

$$\tau(F) \approx \frac{s^{n+3}(F)}{2k_+(F)(s(F) - 1)^2(n(s(F) - 1) - 2)} \approx \frac{s^{n-1}(F)}{2nk_-(F)},$$
(11)

where $s(F) = k_+(F)/k_-(F)$ is the so called stability parameter of the zipper model, i.e. the equilibrium association constant, or affinity, of a single base pair. Eq. 11 is only valid in the limit $s^n(F) \gg 1$ and $s(F) \gg 1$ for the second expression, respectively (Anshelevich et al., 1984). In the opposite limit $s \ll 1$ the dissociation is only determined by the opening process and we expect

$$\tau(F) \approx n/2k_-(F),$$
(12)

because at each of the n opening steps either one or the other end of the zipper can open. The transition at $s \approx 1$ is clearly visible in the loading rate dependence of the unbinding force of zippers with length $n = 10$ and 30 that we calculated by solving Eq. 5 with $F = rt$ numerically and taking the maximum of the distribution Eq. 7. The approximate dissociation time derived from this calculations by Eq. 8 as a function of force is shown in Fig. 5 *A* and compared with the exact mean dissociation time Eq. 6 for $n = 10$. In this numerical example we have chosen the parameters $k_-(0) = 5 \times 10^5 \, \text{s}^{-1}$, $s(0) = 5$ at zero force and $x_{-(+)} = (-)0.05$ nm. They have the order of magnitude of the values extracted from thermodynamic data ($k_- \approx 10^6 \, \text{s}^{-1}$; Pörschke, 1977) and recent force spectroscopic measurements ($x_- - x_+ \approx 0.1$ nm, Strunz et al., 1999). As expected the zipper behaves like a one barrier system in the limit of small forces, i.e. τ decreases to a good approximation exponentially, with a corresponding length scale $x \approx (n - 1)(x_- - x_+) + x_-$ (Eq. 11). The distribution of unbinding forces is also well described by the corresponding distribution Eq. 3 (Fig. 5 *B*). This is no longer true for the strongly forced case ($s \ll 1$) where the dissociation proceeds by n successive opening steps. Because the independent opening steps are governed by the same time scale, the distribution of dissociation times $dN_u(t)/dt$ in Eq. 6 is no longer a single exponential function
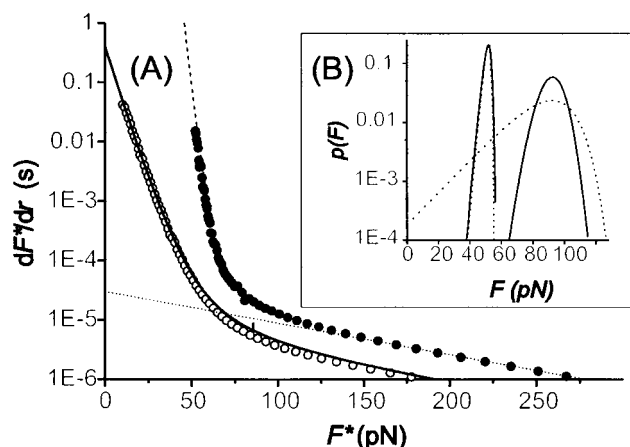
FIGURE 5 (*A*) Approximate mean dissociation time Eq. 8 for a zipper of length $n = 10$ (*open symbols*) and 30 (*closed symbols*) for the model parameters $k_-(0) = 5*10^5$ s^{-1}, $x_- = 0.05$ nm, $k_+(0) = 2.5*10^6$ s^{-1} and $x_+ = -0.05$ nm. The solid curve is the calculated mean dissociation time for $n = 10$. For $n = 30$ the asymptotic behavior according to Eq. 11 for $s > 1$ (*dashed line*) and Eq. 12 is indicated (*dotted line*). (*B*) Force distributions for the two cases $s > 1$ ($r = 1*10^2$ pN/s, $F^* \approx 50$ pN) and $s < 1$ ($r = 1*10^6$ pN/s, $F^* \approx 90$ pN) are given by solid lines for $n = 30$. The dashed lines are the corresponding distributions Eq. 3.

like for the dissociation over a single barrier, but is instead peaked around τ. The successive equivalent opening steps also lead to a much narrower distribution of the unbinding forces (Fig. 5 *B*) compared to the single barrier case, i.e. the width is narrowed by a factor $1/n^{1/2}$ compared to the distribution Eq. 3 and the distribution approaches a Gaussian curve.

The low force regime, i.e. $s > 1$, has been accessed experimentally in the mechanical separation of complementary DNA strands of different length (Strunz et al., 1999). In fact the behavior according to Eq. 11 was observed within the experimental accuracy. A scaling of the length x and the logarithm of the thermal dissociation rate proportional to the number of base pairs, for $n = 10$, 20, and 30, has been found. The transition $s \approx 1$ is, however, not observed in the loading rate-dependent unbinding force experiments because sufficiently high loading rates have not been realized yet.

SUMMARY

We have investigated the forced dissociation kinetics of a ligand-receptor complex in the framework of a network of transition rates, representing the energy landscape of the complex. We have shown that even one intermediate state leads to different, non trivial, dependencies of the bond lifetime on the force. Different transitions dominate the dissociation process at different forces. In general it is not possible to reconstruct the details of the energy landscape from measurements of the bond lifetime; only the slow

transitions determine the lifetime and the lifetime is insensitive to the location of the transition in the binding pocket.

The distribution of dissociation times can deviate markedly from an exponential decay if several transitions take place on the slowest time scale. This typically only occurs at specific forces for one intermediate state or is a consequence of symmetry like in the zipper model. The distribution therefore contains more information about the details of the dissociation process.

We also discussed the experimental observation of the forced dissociation by dynamic force spectroscopy of a single ligand-receptor complex. For the numerical examples, the derivative of the (loading rate-dependent) most probable unbinding force with respect to the loading rate is a good approximation for the mean dissociation time at the unbinding force. The possibility of such measurements has already been demonstrated. However, more details of the underlying energy landscape can only be accessed by accurate measurements of the unbinding force distribution at each loading rate. Because of the present experimental errors and the limited statistics this is still a challenge.

REFERENCES

Abramowitz, M., and I. A. Stegun, editors. 1972. Handbook of Mathematical Functions. Dover Publications, New York.

Allen, S., J. Chen, M. C. Davies, A. C. Dawkes, J. C. Edwards, C. J. Roberts, J. Sefton, S. J. B. Tendler, and P. M. Williams. 1997. Detection of antigen-antibody binding events with the atomic force microscope. *Biochemistry*. 36:7457–7463.

Anshelevich, V. V., A. V. Vologodskii, A. V. Lukashin, and M. D. Frank-Kamanetskii. 1984. Slow relaxation processes in the melting of linear biopolymers: a theory and its application to nucleic acids. *Biopolymers*. 23:39–58.

Balsera, M., S. Stepaniants, S. Izrailev, Y. Oono, and K. Schulten. 1997. Reconstructing potential energy functions from simulated force-induced unbinding processes. *Biophys. J.* 73:1281–1287.

Bell, G. I. 1978. Models for the specific adhesion of cells to cells. *Science*. 200:618–627.

Bongrand, P. 1999. Ligand-receptor interaction. *Rep. Prog. Phys.* 62:912–968.

Carrion-Vasquez, M., A. F. Oberhauser, S. B. Fowler, P. E. Marszalek, S. E. B. Broedel, J. Clarke, and J. M. Fernandez. 1999. Mechanical and chemical unfolding of a single protein: a comparison. *Proc. Natl. Acad. Sci. USA*. 96:3694–3699.

Chang, K. C., and D. A. Hammer. 1999. The forward rate of binding of surface-tethered reactands: effect of relative motion between two surfaces. *Biophys. J.* 76:1280–1292.

Dammer, U., M. Hegner, D. Anselmetti, P. Wagner, M. Dreier, W. Huber, and H.-J. Güntherodt. 1996. Specific antigen/antibody interactions measured by force microscopy. *Biophys. J.* 70:2437–2441.

Dammer, U., O. Popescu, P. Wagner, D. Anselmetti, H.-J. Güntherodt, and G. N. Misevic. 1995. Binding strength between cell adhesion proteoglycanes measured by atomic force microscopy. *Science*. 267:1173–1175.

Evans, E. 1998. Energy landscapes of biomolecular adhesion and receptor anchoring at interfaces explored with dynamic force spectroscopy. *Faraday Discussions*. 111:1–16.

Evans, E., and K. Ritchie. 1997. Dynamic strength of molecular adhesion bonds. *Biophys. J.* 72:1541–1555.

Evans, E., and K. Ritchie. 1999. Strength of a weak bond connecting flexible polymer chains. *Biophys. J.* 76:2439–2447.

Evans, E., K. Ritchie, and R. Merkel. 1995. Sensitive force technique to probe molecular adhesion and structural linkages at biological interfaces. *Biophys. J.* 68:2580–2587.

Florin, E. L., V. T. Moy, and H. E. Gaub. 1994. Adhesion forces between individual ligand-receptor pairs. *Science.* 264:415–417.

Fritz, J., A. G. Katopodis, F. Kolbinger, and D. Anselmetti. 1998. Force mediated kinetics of single P-selectin/PSGL-1 complexes observed by AFM. *Proc. Natl. Acad. Sci. USA.* 95:12283–12288.

Gullingsgrud, J. R., R. Braun, and K. Schulten. 1999. Reconstructing potential of mean force through time series analysis of steered molecular dynamics simulation. *J. Comp. Phys.* 151:190–211.

Grubmüller, H., B. Heymann, and P. Tavan. 1996. Ligand binding: Molecular mechanics calculation of the streptavidin-biotin rupture force. *Science.* 271:997–999.

Haymann, B., and H. Grubmüller. 1999. AN02/DNP-hapten unbinding forces studied by molecular dynamics atomic force microscopy simulations. *Chem. Phys. Lett.* 303:1–9.

Hinterdorfer, P., W. Baumgartner, H. J. Gruber, K. Schilcher, and H. Schindler. 1996. Detection and localization of individual antibody-antigen recognition events by atomic force microscopy. *Proc. Natl. Acad. Sci. USA.* 93:3477–3481.

Hinterdorfer, P., K. Schilcher, W. Baumgartner, H. J. Gruber, and H. Schindler. 1998. A mechanistic study of the dissociation of individual antibody-antigen pairs by atomic force microscopy. 1998. *Nanobiology.* 4:39–50.

Izrailev, S., S. Stepaniants, M. Balsera, Y. Oono, and K. Schulten. 1997. Molecular dynamics study of unbinding of the avidin-biotin complex. *Biophys. J.* 72:1568–1581.

Lee, G. U., L. A. Chrisley, and R. J. Colton. 1994a. Direct measurement of the forces between complementary strands of DNA. *Science.* 266:771–773.

Lee, G. U., D. A. Kidwell, and R. J. Colton. 1994b. Sensing discrete streptavidin-biotin interaction with the atomic force microscope. *Langmuir.* 10:354–357.

Merkel, R., P. Nassoy, A. Leung, K. Ritchie, and E. Evans. 1999. Energy landscapes of receptor ligand bonds explored with dynamic force spectroscopy. *Nature.* 397:50–53.

Moy, V. T., E. L. Florin, and H. E. Gaub. 1994. Intermolecular forces and energies between ligands and receptors. *Science.* 266:257–259.

Pörschke, D. 1977. Elementary steps of base recognition and helix-coil transitions in nucleic acids. *Mol. Biol. Biochem. Biophys.* 24:191–218.

Press, W. H., S. A. Teukolsky, W. T. Vetterling, and B. P. Flannery. 1992. Numerical Recipes in FORTRAN 77. Cambridge University Press, Cambridge.

Rief, M., M. Gautel, F. Oesterhelt, J. M. Fernandez, and H. E. Gaub. 1997. Reversible unfolding of individual titin Ig-domains by AFM. *Science.* 276:1109–1112.

Simson, D. A., M. Strigl, M. Hohenadel, and R. Merkel. 1999. Statistical breakage of single protein A-IgG bonds reveals crossover from spontaneous to force-induced bond dissociation. *Phys. Rev. Lett.* 83:652–655.

Strunz, T., K. Oroszlan, R. Schäfer, and H.-J. Güntherodt. 1999. Dynamic force spectroscopy of single DNA molecules. *Proc. Natl. Acad. Sci. USA.* 96:11277–1182.

Williams, P. M., A. Moore, M. M. Stevens, S. Allen, M. C. Davies, C. J. Roberts, and S. J. B. Tendler. 2000. On the dynamic behavior of the forced dissociation of ligand-receptor pairs. *J. Chem. Soc. Perkin Trans. 2.* 1:5–8.

Zhu, C. 2000. Kinetics and mechanics of cell adhesion. *J. Biomech.* 33:23–33.